COMITATO NAZIONALE PER L'ENERGIA NUCLEARE
Laboratori Nazionali di Frascati

LNF-73/38
27 Giugno 1973

M. Piacentini and G. Strinati: DESIGN OF A SOFT X RAY GRAZING INCIDENCE MONOCHROMATOR FOR SYNCHROTRON RADIATION.-

Servizio Documentazione
dei Laboratori Nazionali di Frascati del CNEN
Casella Postale 70 - Frascati (Roma)

Laboratori Nazionali di Frascati del CNEN
Servizio Documentazione

LNF-73/38
27 Giugno 1973

M. Piacentini(x) and G. Strinati(x): DESIGN OF A SOFT X RAY GRAZING INCIDENCE MONOCHROMATOR FOR SYNCHROTRON RADIATION. -

ABSTRACT. -

Commercial monochromators do not completely match the special characteristics of synchrotron radiation.

In this work we develope a new design for a soft X ray monochromator for synchrotron radiation.

This monochromator offers many advantages: second orders elimination on the whole spectral range, fixed position of the sample, high resolution and remarkable versatility.

INTRODUCTION. -

The synchrotron radiation emitted by the electrons accelerated in the machines built for research in the field of high energy physics, is being used more and more as a light source in the vacuum ultraviolet region (10÷2, 000 Å). The advantages offered by the synchrotron radiation in comparison with conventional light sources is far beyond any discussion[1,2]: its spectral distribution is continuous over a wide spectral range (from X ray to visible and further) and it is peaked in the short wavelengths region, with an intensity some orders of magnitude higher than in the case of conventional sources. Moreover, it

(x) - Istituto di Fisica dell'Università di Roma.

has a high degree of polarization with the electric vector vibrating in the orbital plane of the electrons.

Commercial spectrographs and mono chromators for soft X ray have a concave reflecting grating mounted on the Rowland circle at grazing incidence for dispersing the radiation[3, 4]. But such instruments are not suitable for working with synchrotron radiation. First of all, diffraction gratings working at grazing incidence provide a high efficiency not only in the first order but also at higher orders, so that the overlapping of the higher orders is an unavoidable obstable when measurements are made with a continuous soft X ray source. Secondly, the scanning of wavelengths is performed moving the exit slit along the Rowland circle. This makes it very hard to design experimental chambers complete with vacuum equipment which move along with the exit slit without weighing on it. On the other hand, to mount the sample in front of the entrance slit is not a good solution either because of the possibility of spurious effects or because some kinds of experiments cannot be performed (e. g. electron photoemission). Finally, commercial monochromators are usually designed with a horizontal dispersing plane; such a kind of mounting is not advantageous with synchrotron radiation, which becomes p-polarized with the electric vector vibrating in the plane of incidence, so that its reflectivity is rather low.

Many groups performing research using synchrotron radiation have designed and built monochromators which overcome the difficulties discussed above[5, 6, 7]. The main characteristics of their instruments are:

1) suppression of second orders;
2) fixed directions of the entrance and exit beams as well as fixed slits;
3) vertical plane of reflection and dispersion;
4) as small a number as possible of optical elements.

We have designed a different kind of grazing incidence monochromator for soft X ray based on the following considerations. The Rowland mounting represents the simplest grazing incidence monochromator with the high resolution and the smallest number of optical elements. Such a monochromator, developed in a vertical plane, is "our" actual monochromator. The sample chamber is placed in front of the entrance slit, so that only the detector moves with the exit slit. Before the sample we mount a wide-band filter which selects only a small portion of the total spectral range of the incident radiation, providing therefore the filtering of higher spectral orders. This filter is formed by a plane grating, whose diffracted beam is collected by a spherical mirror and focused on the sample. The whole instrument is actually made of two monochromators in series whose tasks differ. The first one has low resolution and must only cut second orders from the synchrotron spectrum. The second

one must really measure the wavelengths with a high resolving power.

This instrument, designed chiefly for transmission measurements, can also be used for other kinds of experiments, such as fluorescence, in which case the first monochromator selects the fixed wavelength of excitation of the sample, while the second one scans the fluorescence spectrum.

In Fig. 1 we sketch the design of our monochromator[8]. The plane diffraction grating G_1 is illuminated from the synchrotron and the spherical mirror M focuses a portion of the spectrum diffracted by G_1 on the slit S. S corresponds to the entrance slit of the "true" grazing incidence monochromator, in which the concave grating G_2 is mounted on the Rowland circle. The detector F moves on the Rowland circle, while the sample holder T is fixed and placed between M and S. In order to limit the side of the beam coming from the synchrotron (that we assume to be parallel to within a good approximation), an adjustable slit L is placed in front of G_1.

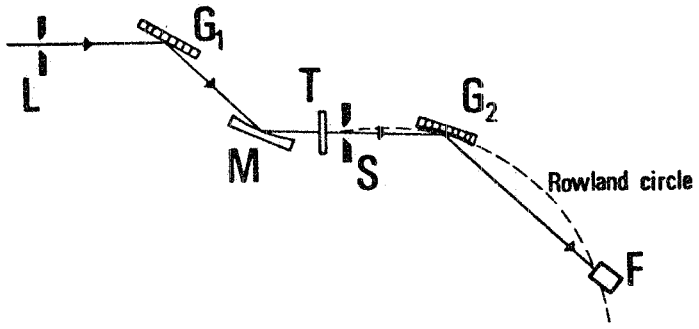

FIG. 1 - Scheme of the proposed monochromator.

In Sec. 1 we recall the main properties of a grating. In Sec. 2 we shall discuss the filter and in Sec. 3 we shall describe the second monochromator. In Sec. 4 we shall discuss the whole mounting while in Sec. 5 we shall examine a practical example.

1. - REMARKS ABOUT GRATING PROPERTIES. -

The diffraction law in the case of a plane grating is:

$$d(\sin\alpha + \sin\beta) = m\lambda \tag{1}$$

where d is the groove separation, α and β are respectively the angles of incidence and diffraction measured from the normal to the grating surface, as shown in Fig. 2, where the angle γ of diffraction inside the grating is also represented. Eq. (1) gives the positions of the prin

cipal maxima of diffraction corresponding to the different orders m for a fixed wavelength λ and a fixed angle of incidence. m may have both positive and negative integer values, corresponding respectively to the inside and the outside spectra.

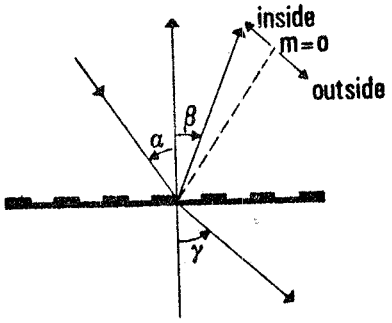

FIG. 2 - Notations and conventions adopted for the diffraction grating.

Eq. (1) holds also for a concave grating if the distance of the source from the Rowland plane is small in comparison with the distance from the grating centre. The concave grating, however, causes some aberrations, the main of which is astigmatism. It can be shown that aberration are dominant at grazing incidence[3] so that care must be taken to lower their contribution in designing a soft X ray monochromator.

1.1. - Resolving power. -

The resolving power of the plane grating is given by:

(2) $$\mathcal{R} \equiv \frac{\lambda}{\Delta\lambda} = |m| N$$

where N is the number of the grooves exposed to the incident radiation.

For the concave grating eq. (2) is modified by a factor depending upon the exposed width of the grating in the limit of a point source[9, 10]. Now, for each wavelength and for each value of the angle of incidence there is an optimum width Wopt for the exposed area of the grating, in correspondence of which the resolving power of the grating reaches a maximum:

(3) $$\mathcal{R}_{opt} = 0.92 \; W_{opt} \frac{|m|}{d} .$$

Wopt depends stronghly on the angle of incidence, decreasing for increasing values of α as well as of β. If the grating is illuminated through a slit of width s, the resolving power of the grating is given by:

(4) $$\mathcal{R}_{slit} = 0.91 \frac{\varrho \lambda |m|}{s d}$$

where ϱ is the radius of curvature of the grating. The calculated resolving power of a monochromator is given by the smaller value that is obtained using either eq. (3) or eq. (4). In the case of a grazing incidence instrument the value of s obtained by $\mathcal{R}_{slit} = \mathcal{R}_{opt}$ are too narrow to be effectively built, so that eq. (4) must be used.

1.2.- Efficiency.-

According to Miller[11], Fujiwara and Iguchi[12], the shortest wavelength which appears in the spectrum of order m is given by $\lambda_c^{(o)}$ in the inside spectrum and by $\lambda_c^{(m)}$ in the outside spectrum, where

$$\lambda_c^{(m)} = \frac{1}{2d\delta}\left[m + \sqrt{m^2 + 4d^2\delta\,(1-\sin\alpha)} \right] . \tag{5}$$

The quantity $\delta = 1/2\,\lambda_p^2$ appears in the expression which approximates the behaviour of the index of refraction n of a material in the soft X ray region, where $\lambda \ll \lambda_p$ (λ_p is the plasma wavelength):

$$n = 1 - \delta\lambda^2 . \tag{6}$$

Since $n < 1$, total reflection occurs for radiation incident on a surface from vacuum, causing a remarkable increase of efficiency. The equations supplied by Fujiwara and Iguchi[12] for calculating the grating reflecting power (i.e. the ratio of the intensity of the beam reflected in order m to the intensity of the incident beam) are difficult to be used even with a large digital computer. We therefore prefer to use the equations supplied in Sprague et al.'s paper[13], whose theory differs from that of Fujiwara and Iguchi[12], giving the cutoff wavelength at $\lambda_c^{(m)}$ in both the inside and the outside spectrum for every value of m.

According to the theory of Sprague et al.[13], assuming the simple groove shape of Fig. 2, in which only a portion w of the groove separation is reflecting, the reflecting power of the diffracted beams in the order m for the two components of polarization parallel (P) and normal (S) to the plane of incidence, is given by:

$$R_P^{(m)} = D_m^2 \left| \frac{n\cos\alpha - \cos\gamma}{n\cos\beta + \cos\gamma} \right|^2 \frac{\cos\beta}{\cos\alpha} \tag{7}$$

$$R_S^{(m)} = D_m^2 \left| \frac{\cos\alpha - n\cos\gamma}{\cos\beta + n\cos\gamma} \right|^2 \frac{\cos\beta}{\cos\alpha} . \tag{8}$$

γ is related to β by:

$$\sin \gamma = \frac{\sin \beta}{n} \quad , \tag{9}$$

and D_m is given by:

$$D_m = (-1)^m \frac{\sin(\pi m w/d)}{\pi m} \quad . \tag{10}$$

In the case of a blazed grating the efficiency increases at the wavelength[3]:

$$\lambda_{Blaze} = \frac{2 d \sin \theta_B}{m} \cos(\alpha - \theta_B) \tag{11}$$

where θ_B is the blaze angle.

2. - THE FILTER. -

2.1. - Optical scheme. -

In Fig. 3 the optical scheme of the first monochromator is shown. The beam coming from the synchrotron can be considered with a good approximation to be formed by parallel rays which are diffracted by the plane grating G_1. The spherical mirror M, of radius ϱ_M, focuses into the slit S the rays diffracted by G_1 in a fixed direction forming an angle C with the incident beam. The wavelength is changed in the simple way by turning G_1 around an axis through its reflecting surface and parallel to the grooves. This kind of mounting is very similar to that of Miyake et al.[7] and imposes that the angle

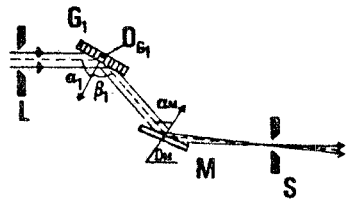

FIG. 3 - Optical scheme of the filter.

$$C = \alpha_1 - \beta_1 \tag{12}$$

is constant.

We have chosen to scan wavelengths in the first order of the outside spectrum for the following reasons:

i) the ratio between the widths of the incident beam to the diffracted beam increases with increasing wavelengths. In this way the decrease

of the spectral distribution of the incident radiation is compensated by the higher concentration of the radiation in the diffracted rays, so that a more uniform diffracted spectral distribution is achieved. Moreover, a narrower beam requires a shorter portion of the reflecting surface on the spherical mirror M, so that the geometrical aberrations produced by a grazing incidence reflection are lowered.

ii) the angle of incidence α_1 decreases for increasing values of the wavelength diffracted by G_1 into the fixed direction $G_1 M$. In this way the cutoff wavelength $\lambda_c^{(m)}$ increases, so that during the scanning one may always be in a good condition for the suppression of second orders.

In fact, the main task of this monochromator is to filter higher orders, instead of using suitable transmission windows.

Let us write explicitely the expressions for the cutoff wavelengths for the first and the second negative orders:

$$\lambda_c^{(-1)} = \frac{\sqrt{1+4 d_1^2 \delta_1 (1-\sin\alpha_1)} - 1}{2 d_1 \delta_1} \tag{13}$$

$$\lambda_c^{(-2)} = \frac{\sqrt{1+ d_1^2 \delta_1 (1-\sin\alpha_1)} - 1}{d_1 \delta_1 / 2} . \tag{14}$$

In Fig. 4 we have plotted eq. (13) (lower curve) and eq. (14) (upper curve) versus α. The area lying between these two curves corresponds to the free spectral range, that is to say the range of wavelengths free from overlapping of higher order light.

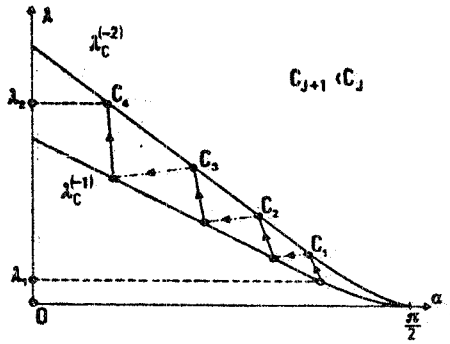

FIG. 4 - Scanning system of the filter between λ_1 and λ_2.

From eq. (12) and choosing $m = -1$, the equation for the plane grating can be rewritten as:

$$\lambda = 2 d_1 \cos\frac{C}{2} \sin\left(\frac{C}{2} - \alpha_1\right). \tag{15}$$

The lower limit of the range of allowed values of α_1 in eq. (15) is determined by the condition $|\beta_1| = \pi/2$ for which the diffracted ray runs along the grating surface, while the upper limit is given by the condition $|\beta_1| = \alpha_1$.

Let us now analyze how we can scan the range of wavelengths $\lambda_1 \div \lambda_2$, always remaining in the free spectral range of G_1. From the

curve of $\lambda_c^{(-1)}$ plotted in Fig. 4 we find the angle $\alpha_{1\,max}^{(I)}$ corresponding to $\lambda_{min}^{(I)} = \lambda_1$ and from eq. (15) we obtain the corresponding value of $C = C^I$. Now we plot eq. (15) on Fig. 4 with $C = C^I$, which intersects the curve of $\lambda_c^{(-2)}$ at the wavelength $\lambda_{max}^{(I)}$. If $\lambda_{max}^{(I)} \geq \lambda_2$, our purpose is achieved. On the contrary if $\lambda_{max}^{(I)} < \lambda_2$, we can obtain our purpose only by moving the grating and the mirror in such a way that the range $\lambda_{max}^{(I)} \div \lambda_2$ falls again in the free spectral range. That is to say, we fix a new value for λ_{min}, we find a new value for C and we scan again to find a new value of λ_{max}. In this way the whole range $\lambda_1 \div \lambda_2$ is divided into several steps, each one corresponding to a different value of C. Each step will be labelled by a parameter j, which increases for increasing wavelengths, and the value of $\lambda_{min}^{(j+1)}$ of the next step is given by:

$$\lambda_{min}^{(j+1)} = 0.9\, \lambda_{max}^{(j)} \qquad j = I, II, III, \ldots \tag{16}$$

in order to overlap the ranges of two successive steps. This process by steps is also shown in Fig. 4.

For m = 0 the grating behaves like a mirror (see eq. (1)), so that also in the case of a mirror we can define a cutoff wavelenght $\lambda_c^{(0)}$ given by eq. (5):

$$\lambda_c^{(0)} = \sqrt{\frac{1-\sin \alpha_M}{\delta}} \tag{17}$$

which corresponds to the shortest wavelenght reflected by the mirror. Also the mirror provides a free spectral range lying between $\lambda_c^{(0)}$ and $2\,\lambda_c^{(0)}$. The angle of incidence α_M on the mirror must be such that the shortest wavelenght diffracted by the grating at each step is also reflected by the mirror. This condition gives:

$$\alpha_M(\lambda_{min}^{(j)}) \geq |\beta_1(\lambda_{min}^{(j)})|. \tag{18}$$

Obviously the direction of the beam reflected by M makes an angle Δi with respect to the direction of the incident beam on G_1. From eq. (18) the relation

$$\Delta i \geq \alpha_M(\lambda_{min}^{(j)}) - \alpha_1(\lambda_{min}^{(j)}) \tag{19}$$

follows, which gives the minimum deviation between the entrance and the exit beams of the filter. At the cutoff wavelength the reflecting powers of the grating and of the mirror actually are not step-like functions but they decrease rather smoothly. Therefore, in order to achieve the best efficiency in filtering light of higher orders we choose as free spectral range of the whole system grating and mirror the one provided by the grating only even if $2\lambda_c^{(0)}(\alpha_M) > \lambda_c^{(-2)}(\alpha_1)$ for each step j.

2.2.- Mechanical motion.-

Within each step j, the only movement required in the filter is a right hand rotation of the grating G_1. Let us now study the motion of G_1 and of M in passing from step j to step j+1. This motion is limited by three conditions:

i) fixed entrance beam;
ii) fixed exit beam;
iii) the mirror must focus on the fixed slit S. The required motions are shown in Fig. 5:

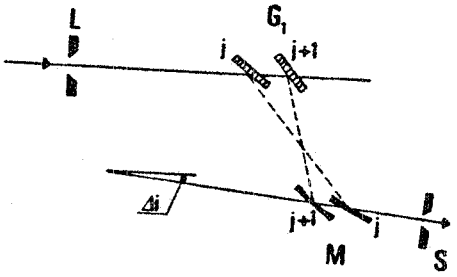

FIG. 5 - Positions of G_1 and M in passing from the step j to the step j+1.

a) the spherical mirror must be turned around an axis through O_M by $(C_j - C_{j+1})/2$ and displaced along the exit beam by:

$$\overline{S'S}_{j \to j+1} = \frac{\varrho_M}{2}\left(\cos \alpha_M^{j+1} - \cos \alpha_M^{j}\right) \tag{20}$$

so that M goes away from S;

b) the grating G_1 must be rotated to a new angle of incidence $\alpha_1(\lambda_{min}^{(j+1)})$ from $\alpha_1(\lambda_{max}^{(j)})$ and must be displaced along the incident beam by:

$$h'_{j \to j+1} = h_{j \to j+1} - \eta_{j \to j+1} \tag{21}$$

where:

$$h_{j \to j+1} = B_j(\operatorname{cotg} C_{j+1} - \operatorname{cotg} C_j) \tag{22}$$

(23) $$\eta_{j \to j+1} = \overline{S'S}_{j \to j+1} \frac{\sin(C_{j+1} + \Delta_i)}{\sin C_{j+1}}$$

(24) $$B_j = B_{j-1} - \overline{S'S}_{j-1 \to j} \sin \Delta_i .$$

The set of values B_j is established once $B_I = a_I \sin C_I$ is fixed, where a_I is the distance $\overline{O_{G_1} O_M}$ in the first step.

3. - THE ROWLAND MONOCHROMATOR. -

The Rowland monochromator is of the standard type, with vertical Rowland plane. The rays coming from the mirror of the filter are focused on the entrance slit of the monochromator and than illuminate the concave grating G_2. Both S and G_2 are fixed during the wavelength scanning, while the exit slit, to which the detector is attached, moves along the Rowland circle. A mask with slits of different width can be set between S and G_2 in order to be in the best conditions for the illumination of the grating.

This monochromator works with the first order inside spectrum in order to decrease the angle of diffraction β_2 and to increase the resolving power. The grating equation of the monochromator is therefore:

(25) $$\lambda = d_2(\sin \alpha_2 + \sin \beta_2)$$

where d_2 is the groove separation of G_2 and α_2 is the angle of incidence on G_2. α_2 must be such that the shortest wavelength provided by the filter is also found at the exit slit of this monochromator. From the cutoff condition of the inside spectrum we have that α_2 can be determined solving the equation:

(26) $$\lambda_1 = \sqrt{\frac{1 - \sin \alpha_2}{\delta_2}} .$$

The astigmatism produced by the concave grating G_2 can be reduced by suitable usage of the focusing mirror M of the filter(3). In fact M can be designed in order to have in S a (nearly) point source provided by it s horizontal focus, and to have in the vertical focal point of the concave grating(x) another point source provided by the vertical focus(o).

(x) e (o) - See pag. 11.

Since the statements imposed on horizontal focusing (by which we fixed ϱ_M) are quite indipendent of the astigmatism decrease, if we want to reconcile the different requirements, it is necessary to use a toroidal mirror whose vertical radius (with the light source at infinity) is given by(8):

$$(27)\quad \varrho_{Mv} = \cos\alpha_M \left[2\,\varrho_{G_2} \left(\cos\alpha_2 - \frac{1}{\cos\alpha_2 - \sin\alpha_2 \tan\beta_2} \right) + \varrho_{Mh} \cos\alpha_M \right]$$

where $\varrho_{Mh} \equiv \varrho_M$.

4. - THE WHOLE MOUNTING. -

In the previous two sections we discussed the elements forming the two monochromators separately. Only by considering all the elements as a single instrument it is possible to fix the values of some of the parameters for the practical mounting.

a) - Radius of curvature of the spherical mirror. -

The choice of the radius of curvature ϱ_{Mh} of the spherical mirror is achieved by taking into account several conditions. First of all, in order to reduce the coma type aberrations of the system composed by M and by G_2, we must have $\varrho_{Mh} \ll \varrho_{G2}$(14, 8). On the other hand, for reducing the geometrical aberrations, we have seen that the mirror should be of the toroidal type. Secondly, the shortest distance of O_M from S occurring in the first step must be small to leave enough space for the sample holder. Finally, in order to achieve the higher resolving power from the second monochromator, the beam reflected by M and focused on S must have such a divergence to fill at least the optimum width W_{opt} of G_2.

b) - Distance between G_1 and M. -

The distance between the plane grating and the spherical mirror must be such that the mirror does not collect the intense tail of the zero order of the grating at wavelnegths near λ_1(15). Its shortest distance can be obtained by(8):

(x) - We remember that "vertical focal point" of a concave grating is a point such that, if we set here a source or its virtual image, we have a stigmatic image on the Rowland circle.

(o) - The words "horizontal" and "vertical" are here referred to the conventional mounting with horizontal Rowland plane.

$$a_1 = \frac{\varrho_M \cos \alpha_M^{(I)}}{2\lambda (d\beta/d\lambda)} \tag{28}$$

where ϱ_M is the illuminated width of the mirror.

c) - Angular deviation of the filter.-

The angle Δi between the entrance beam and the exit beam of the filter has a lower limit given by eq. (19). It has been verified numerically (see the next section) that if we set $\Delta i = \alpha_M(\lambda_{min}^{(I)}) - \alpha_1(\lambda_{min}^{(I)})$, eq. (18) is not satisfied any more in the following steps, even if the variation is so small as to lie in the mechanical errors of the instrument.

d) - Positions of M and G_1.-

The positions of M along the exit beam referred to the slit S are easily determined by the focusing condition:

$$\overline{O_M S}^{(j)} = \frac{\varrho_{Mh}}{2} \cos \alpha_M^{(j)} \tag{29}$$

as soon as the radius ϱ_{Mh} is choosen according to subsection 1. It is more difficult to give the relative positions of the entrance and the exit beams in the filter, which depends on the distance $\overline{O_{G_1} O_M}$. This choice can be made in a graphical way.

e) - Position and radius of G_2.-

The choice of the radius of curvature ϱ_{G_2} of G_2 can be chosen on the basis of reducing aberrations according to subsection 1 and to limit the dimensions of the second monochromator. The condition $\varrho_{Mh} \ll \varrho_{G_2}$, however, is not very restrictive since the relative aperture of M can be chosen very small so that the coma is negligible. At this point all the parameters of this monochromator are determined, because also the angle of incidence α_2 on the grating is known by sec. 3. The distance of the grating from S is given by:

$$\overline{S O_{G_2}} = \varrho_{G_2} \cos \alpha_2 . \tag{30}$$

f) - Resolving power.-

The resolving power of the two monochromators in series is given by[8]:

(31) $$\mathcal{R}_{tot} = \mathcal{R}_2 \left[1 + \frac{\cos(C - \beta_1)}{\cos \beta_1} \right]$$

where $\mathcal{R}_2$ is the resolving power of the Rowland monochromator, given by eq. (4).

Since G_1 works in the outside spectrum, $\cos(C - \beta_1) > \cos \beta_1$, the filter improves the resolving power of the second monochromator at least by a factor two, making it even more uniform over the whole spectral range.

5. - A PRACTICAL EXAMPLE. -

We want now to discuss the design of an effective instrument following the considerations given in the previous sections. Such considerations are quite general and it is sufficient to change the input parameters in order to change the kind of instrument of interest. We now consider a monochromator for scanning the wavelength range $50 \div 250$ A, in order to compare our design with instruments built in other laboratories.

a) - The filter. -

The filter is equipped with a plane grating with 1200 grooves/mm, gold coated. Since we must work in the outside spectrum, a simple rules grating has been chosen, because the effect of blaze is that of concentrating the diffracted radiation into the inside spectrum. Fig. 6 shows the curves for $\lambda_c^{(-1)}$ and $\lambda_c^{(-2)}$ for this grating. The range $50 \div 266$ A is covered in three steps, which are also shown in Fig. 6 by means of the scanning curves. Table I reports the values of the characteristic parameters of each step. The deviation Δi between the entrance and the exit beam is $1^\circ 53'$. The last column of the table gives the quantity $\alpha_M - \beta_1^{min}$, showing that in the second and third step the relation (18) is not any more fulfilled by some hundredths of a degree.

The illuminated area of the grating is $W = s_i / \cos \alpha_1$ where s_i is the height of the incident beam. For $\alpha_1 = \alpha_1(\lambda_1) = 78^\circ 34'$, $W = 5.05$ cm, if $s_i = 1$ cm (Frascati condition at 6 m). On the other hand, by the ratio of the widths of incident to diffracted beams ($s_o / s_i = \cos \beta_1 / \cos \alpha_1$) and by the largest angle of incidence upon M, $80^\circ 27'$, the reflecting surface width of M is 6 cm. If we leave 10 cm for the sample holder, the radius of curvature of the mirror is $\varrho_{Mh} = 120$ cm, so that the relative aperture is 1/20. The distance $O_{G_1} O_M (I) = a_{(I)}$ must be larger than 12.5 cm. In order not to have too large system dimensions, a possible "good" value for a_I is 20 cm from which all the parameters relative to the first step of the filter are fixed, and consequently through eq. (20), (21), (22), (23) and (24) also for the other steps. In Table II we report the result

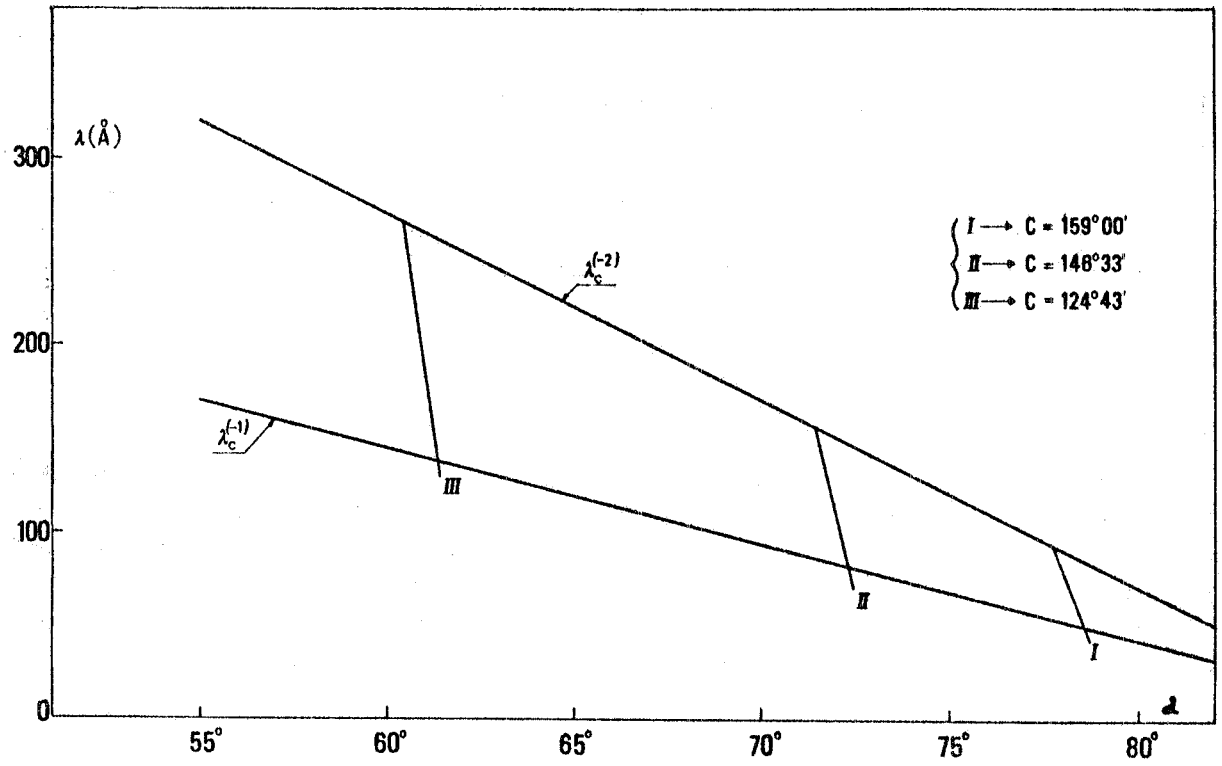

FIG. 6 - Scanning curves of the filter in the range 50÷266 Å.

TABLE I

Characteristic parameters for the filter using a 1200 grooves/mm gold coated plane grating.

J	Spectral range	Range of angle of incidence α_1	C	α_M	$\lvert \alpha_M - \beta_1(\lambda_{min}) \rvert$
I	50.00÷ 91.40 Å	78°34'÷ 77°45'	159°00'	80°27'	0°00'
II	82.00÷156.00 Å	72°18'÷71°24'	146°33'	74°13'	0°02'
III	138.00÷266.00 Å	61°21°÷60°24'	124°43'	63°19'	0°05'

of the calculation, while the places occupied step by G_1 an M are stetcked in Fig. 7.

TABLE II

Values of displacements of G_1 and M.

J	$h'_{j \to j+1}$	$\overline{S'S}_{j \to j+1}$
I	+1.78 cm	6.35 cm
II	-4.68 cm(x)	10.63 cm

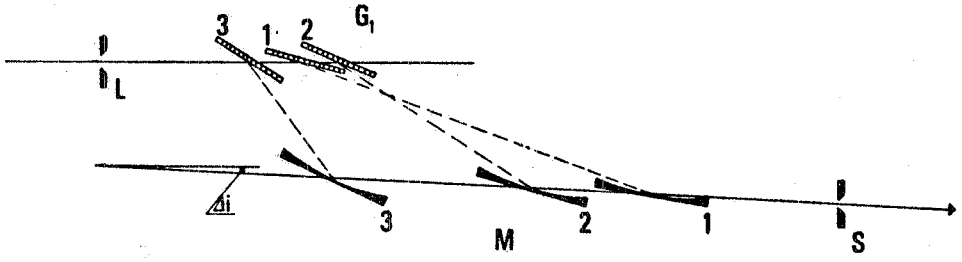

FIG. 7 - Map of the filter for scanning the range 50 ÷ 266 Å.

b) - The second monochromator.-

Since the relative aperture of the mirror is rather small, we choose a 3 m radius grating gold coated (from Bausch & Lomb catalog) with a blaze angle of $2^{\circ}35'$ and 1200 grooves/mm. The angle of incidence is $80^{\circ}27'$ which gives a blaze wavelength at 157 Å.

In Table III are reported the values of ϱ_{Mv} computed from eq. (27) when the mirror M is of the toroidal type. Since ϱ_{Mv} greatly differs step by step, two ways are possible. We can have many mirrors, one for every value of ϱ_{Mv}, replacing each other step by stey, or, since astigmatism is greatest at grazing incidence, we can choose the value

(x) - The values of $h'_{j \to j+1}$ are taken positive in the direction of the incident radiation.

of ϱ_{M_V} corresponding to j = I and accept the astigmatism in steps with j > I.

TABLE III

Values of the vertical radius ϱ_{M_V} of the toroidal mirror M.

J	λ	ϱ_{M_V}
I	50 Å	41 cm
II	92 Å	96 cm
III	160 Å	145 cm

c) - Efficiency.-

The theoretical computation of the efficiency is rather approximate. In Fig. 8 the reflecting power of the plane grating is plotted versus λ for the three steps according to Sprague et al. (computed by Rs only) assuming w = 0.2157.

The gold coated mirror M reflects only 40, 50 and 20% in the three steps[16].

More difficult is the computation for the second monochromator since Sprague's formulas give zero efficiency for $\lambda < \lambda_c^{(o)}$. In Fig. 9 we plot $R_s^{(o)}$ and $R_s^{(+1)}$ of G_2 versus λ, assuming again w = 0.2157. In Fig. 10 is given the total efficiency of the whole instrument.

d) - Resolving Power.-

For a 3 m concave grating with angle of incidence $\alpha_2 = 80^o 2' 7''$ if we let $\mathcal{R}_{slit} = 0.1\ \mathcal{R}_{opt}$, the values of the width s of the entrance slit cover the range $5.4 \div 19.0\ \mu$, which can actually be built. In Fig. 11 we plot $\mathcal{R}_{slit}$ versus λ (● curve) and we show the filter really improves $\mathcal{R}_{slit}$ at least by a factor two (▲ curve).

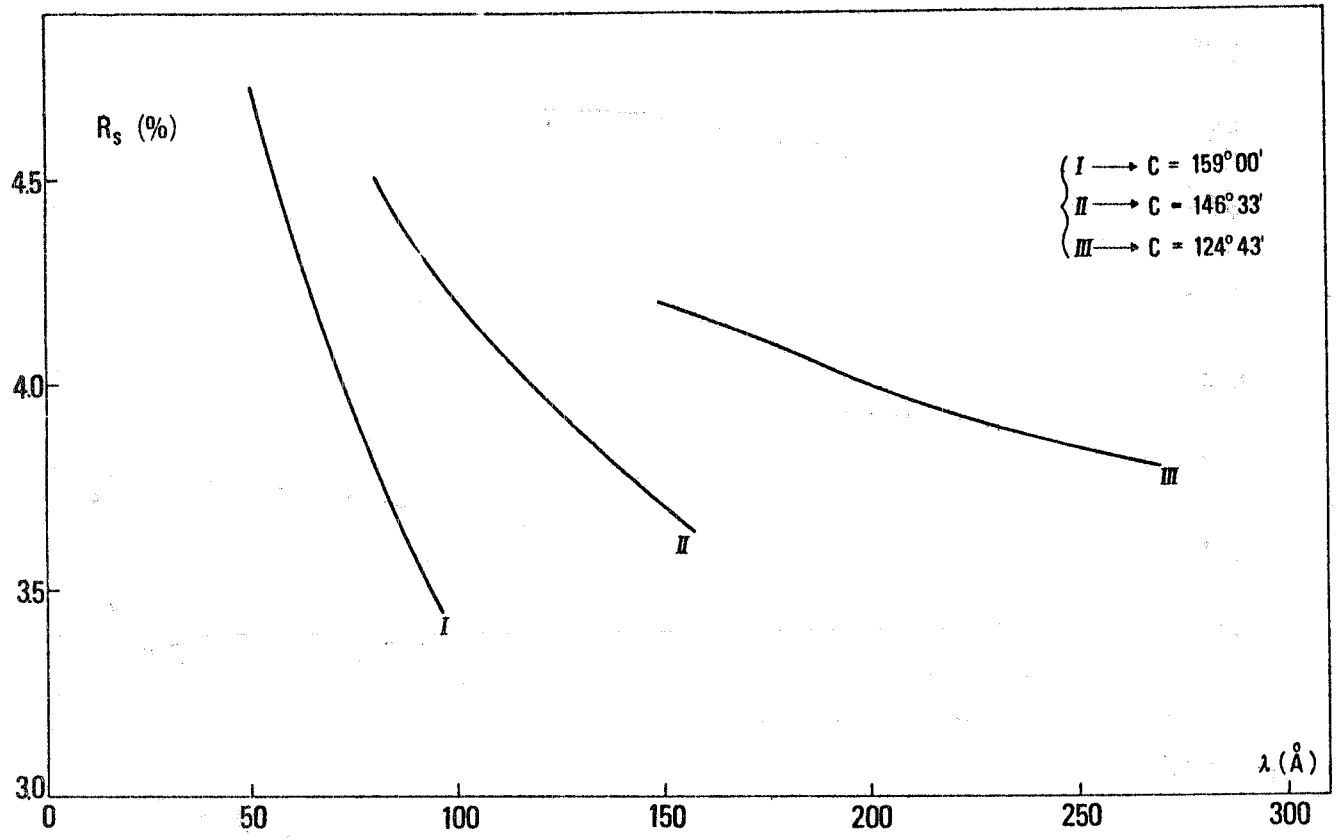

FIG. 8 - Reflecting power of G_1 versus λ.

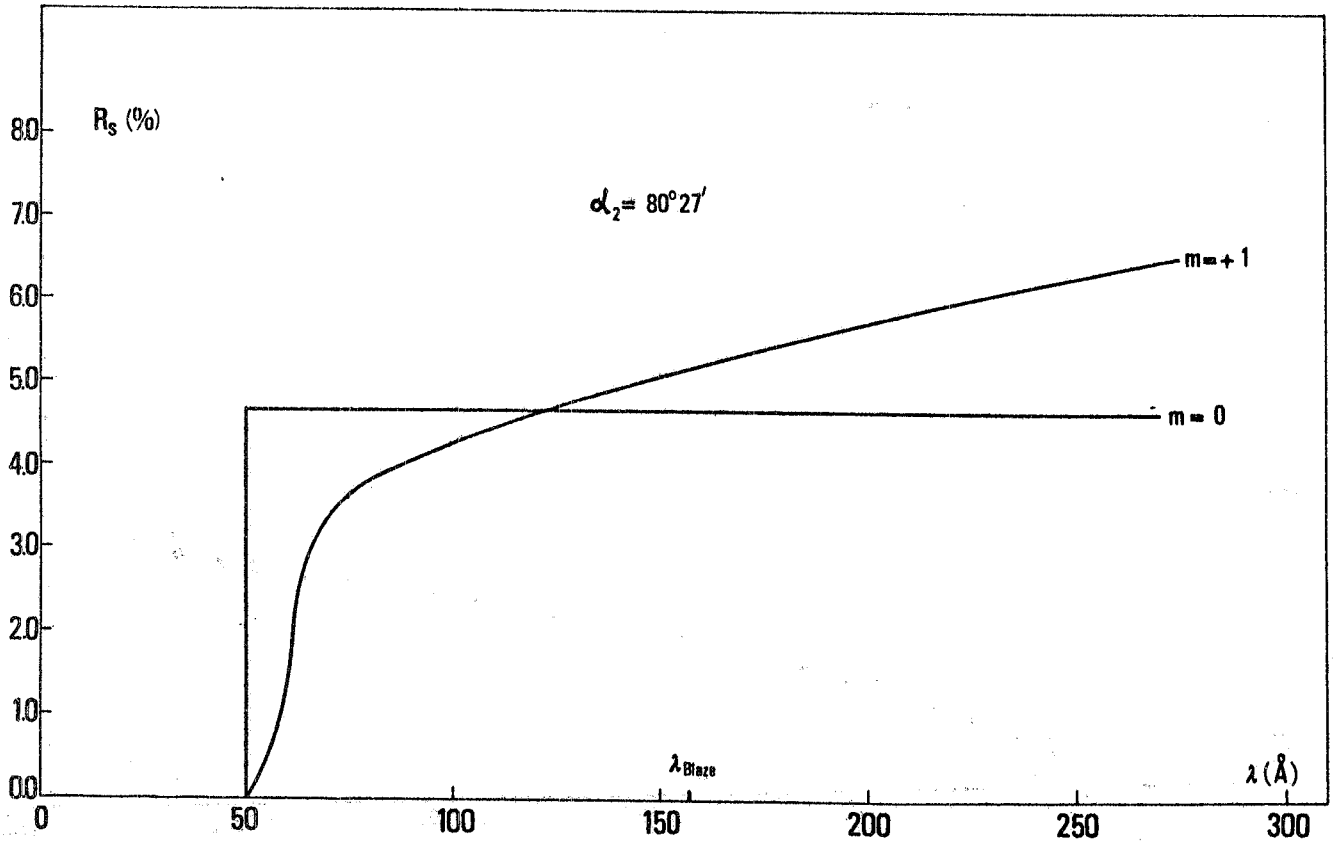

FIG. 9 - Reflecting power of G_2 versus λ.

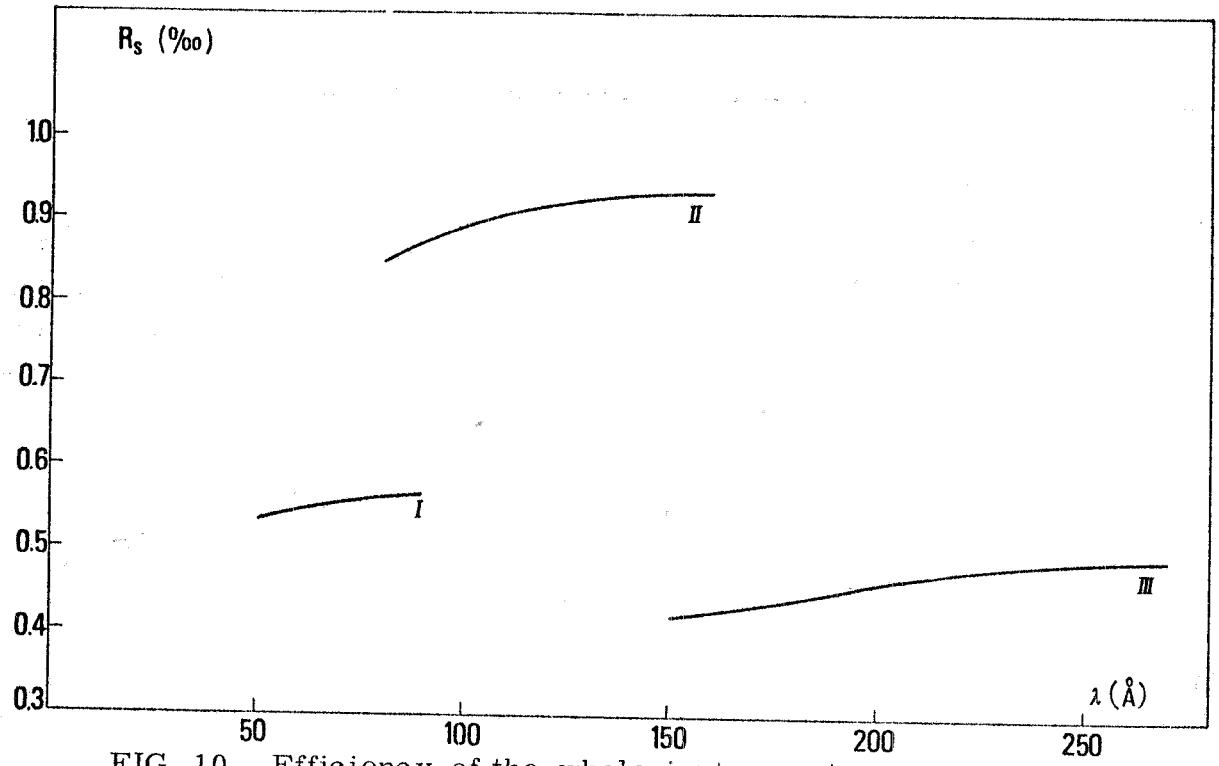

FIG. 10 - Efficiency of the whole instrument.

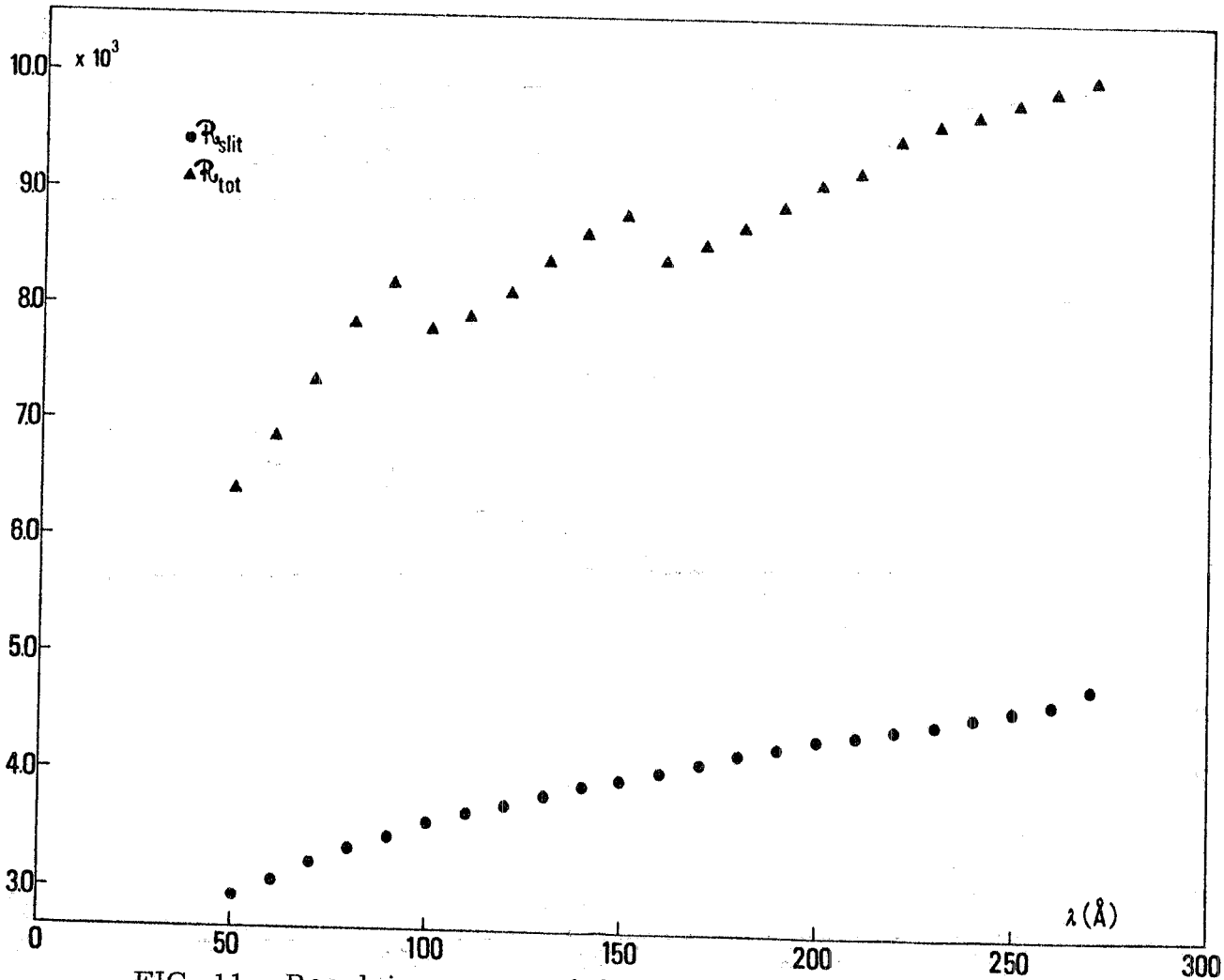

FIG. 11 - Resolving power of the Rowland monochromator (● curve) and of the whole instrument (▲ curve).

REFERENCES. -

(1) - D.H. Tomboulian and P.L. Hartman, Phys. Rev., 102, 1423 (1956).
(2) - A. Balzarotti, L. Bartolini, A. Bianconi, E. Burattini, M. Grandolfo, R. Habel and M. Piancentini, Frascati Report LNF-72/98 (1972).
(3) - J.A.R. Samson, Techniques of Vacuum Ultraviolet Spectroscopy (Wiley & Sons, New York 1967).
(4) - A.N. Zaidel' and E. Ya. Shreider, Vacuum Ultraviolet Spectroscopy (Ann. Arbor, London 1970).
(5) - C. Kunz, Proceedings of the International Symposium for Synchrotron Radiation Users (Daresbury, 1973), to be published.
(6) - H. Dietrich and C. Kunz, Rev. Sci. Instr. 43, 434 (1972).
(7) - K.P. Miyake, R. Kato and H. Yamaschita, Sci. Light 18, 39 (1969).
(8) - G. Strinati, undergraduate thesis, University of Rome (unpublished).
(9) - J.E. Mack, J.R. Stenh and B. Edlen, J. Opt. Soc. Am. 22, 245 (1952).
(10) - T. Namioka, J. Opt. Soc. Am. 49, 446 (1959); 51, 4 (1961).
(11) - J.C. Miller, J. Opt. Soc. Am., 54, 353 (1964).
(12) - S. Fujiwara and Y. Iguchi, J. Opt. Soc. Am., 58, 361 (1968), 58, 1189 (1968).
(13) - G. Sprague, D.H. Tomboulian and D.E. Bedo, J. Opt. Soc. Am. 45, 756 (1955).
(14) - T. Namioka and M. Seya, Applied Optics, 9, 459 (1970).
(15) - R. Kato, private comunication.
(16) - A.P. Lukirskii, E.P. Savinov, O.A. Ershov, I.I. Zhukova and V.A. Fomichev, Opt. Spectry, 19, 237 (1965).